Applied Catalysis B: Environmental 91 (2009) 449–459

Contents lists available at ScienceDirect

Applied Catalysis B: Environmental

journal homepage: www.elsevier.com/locate/apcatb

Porous clay heterostructures (PCHs) intercalated with silica-titania pillars and modified with transition metals as catalysts for the DeNO*x* process

Lucjan Chmielarz [a,*], Zofia Piwowarska [a], Piotr Kuśtrowski [a], Barbara Gil [a], Andrzej Adamski [a], Barbara Dudek [a], Marek Michalik [b]

[a] *Jagiellonian University, Faculty of Chemistry, Ingardena 3, 30-060 Kraków, Poland*
[b] *Jagiellonian University, Institute of Geological Sciences, Oleandry 2a, 30-063 Kraków, Poland*

ARTICLE INFO

Article history:
Received 16 February 2009
Received in revised form 12 June 2009
Accepted 18 June 2009
Available online 24 June 2009

Keywords:
Porous clay heterostructures (PCHs)
Montmorillonite
Silica-titania pillars
DeNOx
Ammonia

ABSTRACT

Porous clay heterostructures (PCHs) intercalated with silica as well as silica-titania pillars were obtained from natural montmorillonite. The PCH samples were modified with copper or iron by an ion-exchange method. Detailed characterization of the obtained materials included: chemical (EPMA), structural (XRD) and textural (BET) analysis, determination of coordination and aggregation of transition metal species (UV–vis-DRS, EPR) as well as analysis of surface acidity (FT-IR, NH_3-TPD). Titanium incorporated into the silica pillars was present mainly in the form of separated cations. Small contribution of polymeric titanium oxides was detected only for the samples with the higher Ti loading. Titanium incorporated into the silica pillars significantly increased the surface acidity of the PCH materials. Transition metals (Cu, Fe) deposited on the surface of PCHs were present mainly in the form of isolated cations and oligomeric metal oxide species. Ti-containing PCHs modified with transition metals was found to be active and selective catalysts of the DeNO*x* process. The Cu- and Fe-modified catalysts effectively operated in a broad temperature range of 350–550 °C and 300–500 °C, respectively. The PCH based catalysts were only slightly deactivated by water vapour and SO_2.

1. Introduction

Air pollution with nitrogen oxides (NO_x) is nowadays one of the major environmental problems. The removal of NO_x in flue gases emitted from stationary (e.g. power plants) as well as mobile (e.g. cars, airplanes) sources remains an important environmental issue. The selective catalytic reduction of NO_x by ammonia (NO_x-SCR, DeNO*x*) is the most widely used process for the elimination of nitrogen oxides emitted by stationary sources. Recently, the modified version of this process using urea solution as a source of ammonia, was applied for the elimination of NO_x emitted by Diesel car engines [1]. The commercial, V_2O_5-TiO_2 based catalysts of the DeNO*x* process dedicated for stationary sources effectively operate in the narrow temperature range of 300–400 °C. Therefore, the search for the new catalytic systems, which could operate in the much broad temperature range and additionally would be cheaper and less or even non-toxic is still continued.

Modified cationic layered clay minerals seem to be very interesting materials for the preparation of the DeNO*x* catalysts. The cationic layered clays can be transformed into the highly porous structures by exchanging interlayer charge compensating cations with large inorganic polymeric oxy–hydroxy cationic species, propping open the silicate layers. Upon calcination the oligomers undergo dehydratation and dehydroxylation, forming nanoparticles of metal oxides which link permanently the silica layers. Such modification of cationic layered minerals results in a formation of microporous materials called pillared interlayered clays (PILCs). Successful pillaring of smectites with Al_2O_3, TiO_2, ZrO_2, Fe_2O_3 and Cr_2O_3 was patented in the late seventies and early eighties of the last century [2–4]. Such pillared smectites [5] as well as their modifications with various transition metals have been found to be active and selective catalysts of the DeNO*x* process [e.g. [6–10]]. Our previous studies have shown a very good catalytic performance of titania pillared montmorillonites doped with copper [11] or iron [12], which selectively operated in the relatively broad temperature range. Unfortunately, the structure of pillared smectites is not stable at temperatures exceeding 500 °C and therefore the application of these catalysts for the high temperature DeNO*x* process is excluded. In 1995 Galarneau et al. [13] proposed a different way to obtain thermally stable porous materials from the cationic layered clays. The synthesis of this new class of materials, which are called porous clay heterostructures

* Corresponding author. Tel.: +48 126632006; fax: +48 126340515.
E-mail address: chmielar@chemia.uj.edu.pl (L. Chmielarz).

0926-3373/$ – see front matter © 2009 Elsevier B.V. All rights reserved.
doi:10.1016/j.apcatb.2009.06.014

(PCHs), is based on the introduction of the silica pillars into the interlayer space of clays by the surfactant directed method. The PCH materials are characterized by high surface area, combined microporous and mesoporous structure, surface acidity and cation exchange properties. The structure of PCHs is stable up to temperatures exceeding 800 °C and therefore these materials can be used in the high temperature processes. Our previous studies have shown the high catalytic activity and stability of Cu- and Fe-modified PCHs obtained from synthetic saponite in the DeNO*x* process [14]. Recently, these observations were extended for PCHs based on natural montmorillonite and vermiculite [15]. It should be noted that all the previously presented studies were performed using silica intercalated PCHs. On the other hand our studies of the PILCs based catalysts showed that their activity in the DeNO*x* process could be improved by incorporation of titania into the structure of pillars. Therefore, we decided to incorporate titanium into the silica pillars in the PCH samples and after their modifications with copper and iron, test these materials in the role of the DeNO*x* catalysts.

2. Experimental

2.1. Materials

Natural montmorillonite (CEC = 82 meq/100 g, S&B Industrial Minerals GmbH) was used as a starting material for the preparation of a series of Ti-containing PCHs. The synthesis of the PCH materials consisted of the following steps: (i) transformation of the parent montmorillonite into the sodium form (Na-Mont) by treatment of the raw clay with a NaCl solution (1.0 M); (ii) exchange of the interlayer sodium cations in Na-Mont for alkylammonium surfactants (0.1 M solution of hexadecyltrimethylammonium chloride (HDTMA, Fluka), 50 °C, 24 h); (iii) separation of the modified clay from solution, washing with demineralised water (till pH = 7) and drying; (iv) introduction of HDTMA-Mont into melted hexadecylamine (HDA, Fluka), which played a role of co-surfactant; (v) addition of the mixture of tetraethylorthosilicate (TEOS, Fluka) and titanium isopropoxide (TIP, Fluka) into the suspension and then stirring at 60 °C for 4 h; (vi) separation of the samples from the solutions, washing with pure ethanol and drying at room temperature; (vi) calcination of the samples at 600 °C for 6 h. The following molar ratios of HDTMA/HDA/TEOS/TIP were applied: 1/20/150/0, 1/20/148.5/1.5, 1/20/142.5/7.5 and 1/20/135/15 for the production of the samples, which respectively are denoted as PCH, PCH-1.5Ti, PCH-7.5Ti and PCH-15Ti. Detailed description of the method used for the preparation of the PCH materials was presented in our previous paper [16].

Transition metals (Cu and Fe) were deposited on the PCH supports by an ion-exchange method using aqueous solutions (0.02 M) of $Cu(NO_3)_2{\cdot}3H_2O$ or $Fe(NO_3)_3{\cdot}9H_2O$. The slurry of 2 g of the PCH sample in 200 ml of nitrate metal solution was stirred at 60 °C for 3 h. Then, the solid was separated by filtration, washed and oven dried at 120 °C for 12 h. The samples modified with copper and iron were dried at room temperature and then calcined in the air atmosphere at 600 °C for 6 h.

2.2. Catalysts characterization

Chemical compositions of the samples were determined by electron microprobe analysis performed on a JEOL JCXA 733 superprobe (electron probe microanalysis–EPMA).

The X-ray diffraction patterns of the raw clay as well as its modifications were obtained with a Philips X'Pert APD diffractometer using Cu K_α radiation.

Scanning electron microscope (SEM) images were obtained on a HITACHI S-4700 equipped with microanalysis system NORAN Vantage operated an accelerating voltage of 20 kV.

Textural parameters of the samples were determined by N_2 sorption at −196 °C using an ASAP 2010 (Micromeritics) automated gas adsorption system. Prior to the analysis, the samples were outgassed under vacuum at 200 °C for 16 h. The surface area was determined using the BET model while distribution of mesopores was calculated using the BJH model. Adsorption branch of isotherm was used for the determination of the mesopore size distribution.

The type and aggregation of transition metals present in the PCH based catalysts was studied by UV–vis-DR spectroscopy. The measurements were performed in the range of 190–900 nm with a resolution of 2 nm using an Evolution 600 (Thermo) spectrophotometer.

X-band CW-EPR spectra were recorded at liquid nitrogen temperature (77 K) with a Bruker ELEXSYS E-500 spectrometer, operating at a 100 kHz field modulation.

The surface acidity of the clay materials was studied by adsorption of pyridine, followed by IR spectroscopy (Bruker Tensor 27). Detailed description of these experiments was presented in our previous papers [15,16]. Additionally, temperature programmed desorption of ammonia (NH_3-TPD) was done for the selected samples. Adsorption of ammonia was performed for the outgases samples (550 °C/1 h) or the catalysts pretreated with water vapor (5% H_2O in He, 200 °C/1 h). Detailed description of the NH_3-TPD experiments was presented in our previous papers [e.g. [11,12,17]].

2.3. Catalytic tests

The modified PCH samples were studied as catalysts for the selective reduction of NO with ammonia (NO-SCR, DeNO*x*). The catalytic experiments were performed in a fixed-bed flow reactor

Table 1
Chemical composition and textural parameters of sodium form of montmorillonite Na-Mont) and the PCH samples.

Sample	Na_2O	K_2O	MgO	CaO	Al_2O_3	SiO_2	TiO_2	Fe_2O_3	CuO	S_{BET} (m^2/g)	V_p (cm^3/g)
Na-Mont	2.37	1.03	1.60	0.80	21.91	69.15	0.11	3.03	0.00	77	0.11
PCH	0.28	0.12	0.66	0.00	9.98	87.44	0.05	1.49	0.00	675	0.49
PCH-Cu	0.05	0.05	0.48	0.00	9.70	86.08	0.05	1.40	2.19	653	0.43
PCH-Fe	0.04	0.05	0.50	0.00	9.72	83.14	0.03	7.00	0.00	640	0.41
PCH-1.5Ti	0.14	0.13	0.72	0.00	12.59	82.06	2.37	1.99	0.00	587	0.45
PCH-1.5Ti-Cu	0.05	0.05	0.46	0.00	12.25	81.13	2.16	1.83	2.07	570	0.41
PCH-1.5Ti-Fe	0.03	0.02	0.79	0.00	12.40	77.47	2.15	7.14	0.00	550	0.40
PCH-7.5Ti	0.51	0.05	1.07	0.08	14.89	76.89	4.68	1.82	0.00	573	0.37
PCH-7.5Ti-Cu	0.20	0.12	0.82	0.00	14.61	76.41	4.62	1.75	1.97	541	0.32
PCH-7.5Ti-Fe	0.30	0.18	0.83	0.00	13.88	72.71	4.48	7.61	0.00	525	0.29
PCH-15Ti	0.39	0.00	1.13	0.00	16.19	71.69	8.43	2.30	0.00	390	0.27
PCH-15Ti-Cu	0.05	0.00	0.40	0.00	15.67	71.51	8.18	2.09	2.10	372	0.23
PCH-15Ti-Fe	0.00	0.00	0.16	0.00	14.16	70.74	7.79	7.15	0.00	348	0.21

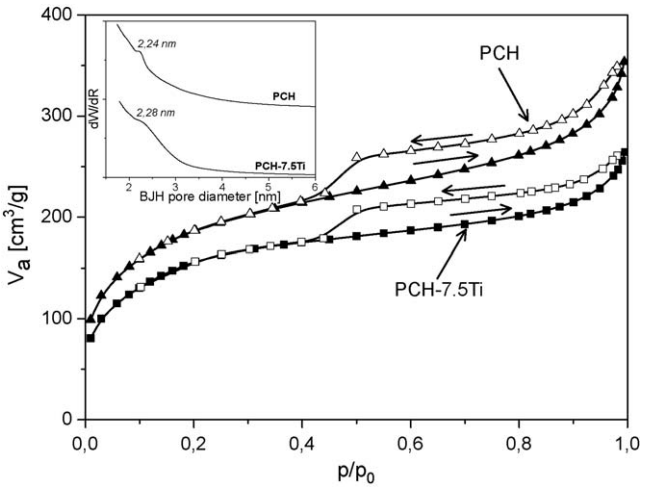

Fig. 1. Examples of adsorption–desorption isotherms and BJH pore size distributions obtained for the PCH and PCH-7.5Ti samples.

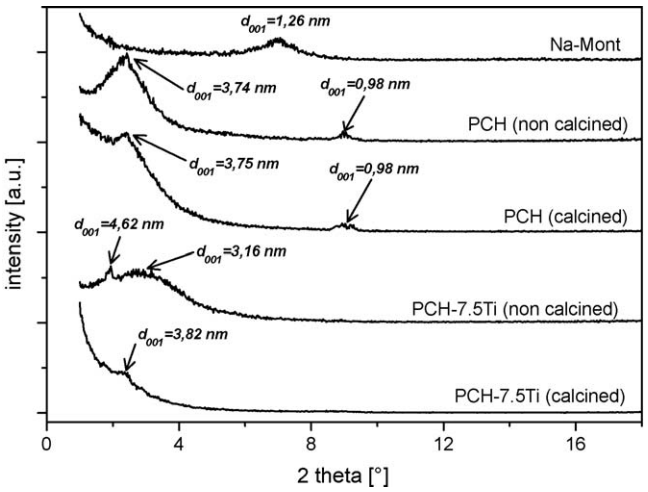

Fig. 2. Examples of X-ray diffractograms of the parent clay, as prepared PCHs and calcined PCHs.

system. The reactant concentrations were continuously measured using a quadrupole mass spectrometer (VG QUARTZ) connected directly to the reactor outlet. Prior to the reaction, each sample (100 mg) of the catalyst was outgassed in a flow of pure helium at 550 °C for 30 min. The following composition of the gas mixture was used: [NO] = [NH_3] = 0.25%, [O_2] = 2.5%. Helium was used as a balancing gas at a total flow rate of 40 ml/min.

The influence of H_2O on the NO-SCR reaction was studied by a periodical addition of water vapor into the reaction mixture (5.0, vol.%). Helium (used as a balance gas) was switched by means of a 4-port valve from dry to wet conditions in intervals of 30 min.

The influence of SO_2 on the catalytic performance was determined by treatment of the samples in flow of SO_2 (2000 ppm) diluted in helium (20 ml/min) in isothermal conditions for 1 h. Comparison of the NO conversion and selectivity to N_2 before and after the treatment of the catalyst with SO_2 allowed evaluating its resistance to the poisoning by sulfur dioxide.

Detailed description of the conditions of the catalytic measurements was presented in our previous paper [15].

Additionally, the stability of the selected catalysts was tested in isothermal conditions (450 °C) using dry ([NO] = [NH_3] = 0.25%, [O_2] = 2.5%) or wet ([NO] = [NH_3] = 0.25%, [O_2] = 2.5%, [H_2O] = 5.0%) reaction mixture.

3. Results and discussion

The chemical composition of montmorillonite (sodium form) and the PCH samples as well as their textural parameters are presented in Table 1. The montmorillonite layers consist of the octahedral alumina sheet sandwiched between two tetrahedral

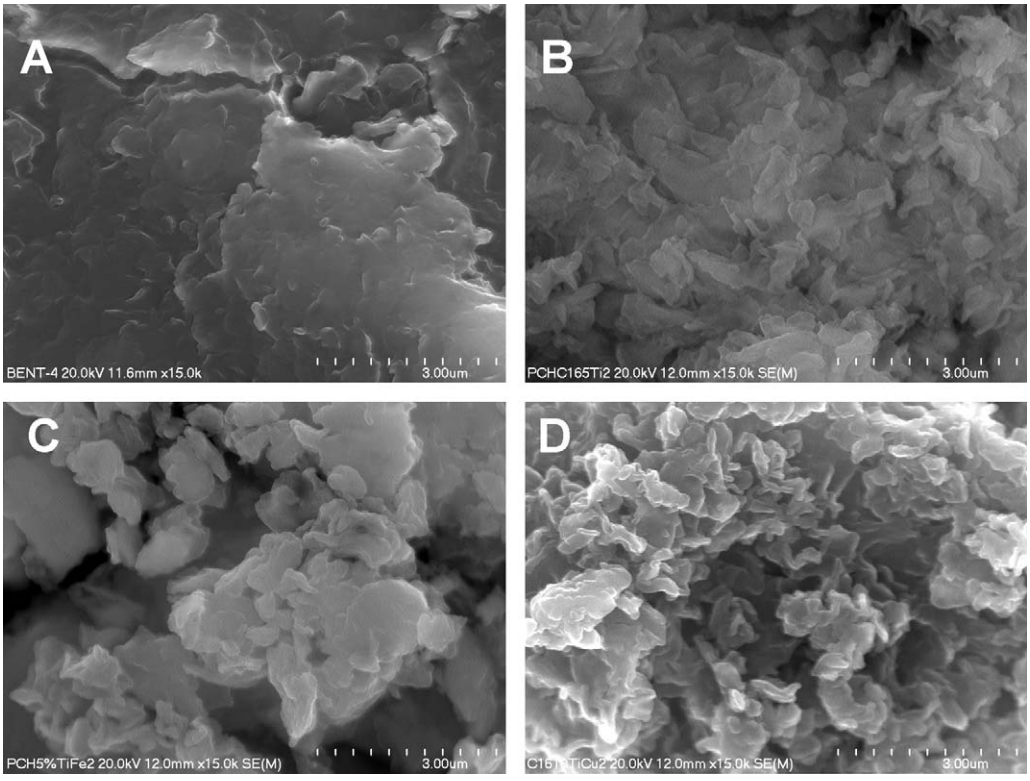

Fig. 3. SEM micrographs of raw montmorillonite (A), PCH-7.5Ti (B), PCH-7.5Ti-Fe (C) and PCH-7.5Ti-Cu (D).

silica sublayers. Therefore, Al_2O_3 and SiO_2 are the main components of the clay. A part of Al^{3+} cations located in the octahedral sheets is substituted by Mg^{2+}, Fe^{3+} and Ti^{4+} ions. The latter two can be also substituted for silica in tetrahedral sheets, however as it was shown in our previous paper [15] the majority of iron cations is located in the octahedral sublayers. Na^+, K^+, Ca^{2+} and possibly also Mg^{2+} cations are located in the interlayer space of montmorillonite and compensate the negative charge of the clay layers. The content of the interlayer cations was significantly reduced in the PCH samples due to their exchange for hexadecyltrimethylammonium ions. The deposition of the silica or silica-titania pillars into the interlayer space of the clays significantly enhanced the content of SiO_2 and TiO_2 in the PCH materials.

The examples of the nitrogen sorption–desorption isotherms as well as BJH pore size distributions (calculated from the adsorption branches of the isotherms) for PCH and PCH-7.5Ti are presented in Fig. 1. A gradual increase in nitrogen sorption observed at low to medium partial pressure ($p/p_0 < 0.3$) suggests the presence of supermicropores and small mesopores. An increase in the adsorbed volume observed at higher partial pressures is related to the presence of larger mesopores. The hysteresis loops could be qualified to the H4 type, corresponding to the presence of the slit-like pores [18]. The BET surface areas (S_{BET}) and pore volumes (V_p) of PCHs and sodium form of montmorillonite are compared in Table 1. Transformation of montmorillonite into PCHs increased its surface area and porosity by nearly one order of magnitude. The highest values of these parameters were found for the PCH sample, while an introduction of titanium into the PCH structure resulted in a gradual decrease in S_{BET} and V_p. Deposition of transition metals (Cu, Fe) on the surface of PCHs only slightly reduced their textural parameters.

The examples of the X-ray diffractograms recorded for the sodium form of montmorillonite (Na-Mont) as well as non-calcined and calcined PCH and PCH-7.5Ti are shown in Fig. 2. The (0 0 1) diffraction peak attributed to the ordering of the clay layers in the Na-Mont sample was found in the position related to the basal spacing of 1.26 nm. The deposition of surfactants and co-surfactants as well as the formation of the silica or silica-titania pillars in the interlayer space of montmorillonite resulted in a shift of the (0 0 1) peak to 2Θ angle of 2.42°, which is related to the basal spacing of 3.74 nm. Taking into account that the thickness of the montmorillonite layer is about 0.96 nm [19,20], it could be calculated that the interlayer distance increased from 0.30 to 2.78 nm. Additionally, the (0 0 1) peak related to the stacked together clay layers ($d_{0\,0\,1}$ = 0.98 nm) was detected. Calcination of the sample only slightly changed the positions of the basal peak but its intensity was significantly reduced. This effect is related to the partial delamination of the PCH structure (non-parallel ordering of the clay layers). Very similar results were obtained for PCH-1.5Ti (not shown). For the samples containing larger amount of titanium (PCH-7.5Ti and PCH-15Ti), the intercalation of surfactants, co-surfactants and precursors of the inorganic pillars (TEOS, TIP) into the interlayer space of montmorillonite also resulted in an expanding of its basal spacing. For PCH-7.5Ti, a broad maximum centred at about 2.78° ($d_{0\,0\,1}$ = 3.16 nm) and sharp peak at 1.92° ($d_{0\,0\,1}$ = 4.62 nm) were found. The interlayer distances related to these peaks are 2.20 and 3.66 nm, respectively. Similar XRD diffractograms were recorded for PCH-15Ti. Obtained results suggest the formation of various aggregates of surfactants, co-surfactants and possibly also precursors of the inorganic pillars (TEOS, TIP) in the interlayer space of the clay. Calcination of the PCH-7.5Ti and PCH-15Ti samples resulted in a formation of the disordered pillared structure (delaminated structure).

The SEM micrographs, presented in Fig. 3, have been recorded in order to get insight into the particles morphology. For the raw montmorillonite (Fig. 3A) large aggregates of platelets mixed with small particles were observed. Intercalation of the silica or silica-titania pillars into the interlayer space of the clay significantly modified its morphology (Fig. 3B). It this case irregularly shaped small aggregates of platy particles were detected. Similar morphology was reported for delaminated Al-PILCs by L.V. Duong et al. [21]. As it was shown by XRD studies the PCH materials were

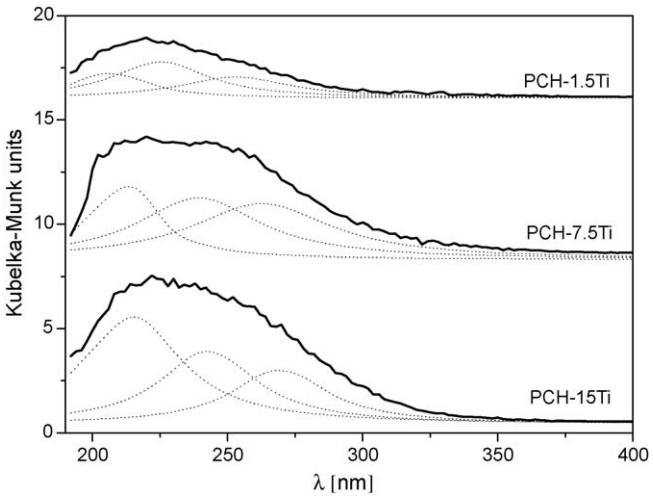

Fig. 4. Differential UV–vis-DR spectra recorded for the Ti-modified samples.

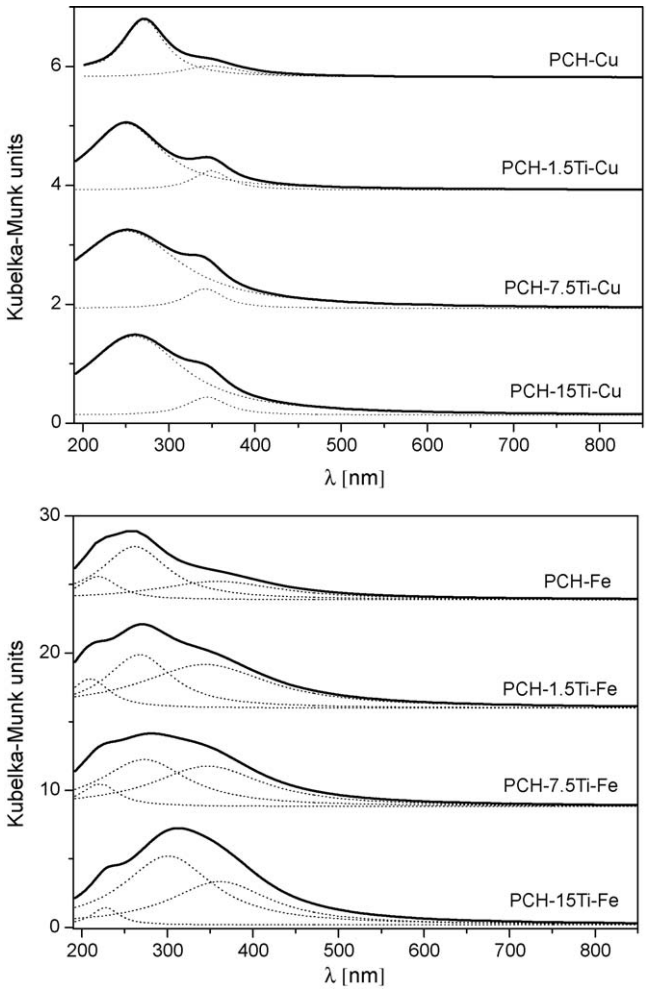

Fig. 5. Differential UV–vis-DR spectra recorded for the samples doped with copper and iron.

also characterized by the delaminated structure. The separated grains of TiO_2 or SiO_2 were not detected by additional analysis (EPMA) in a series of silica or silica-titania pillared clays. Also separated grains of iron or copper oxides were not detected in the PCH samples doped with these transition metals. The obtained results are supported by XRD analysis, which have not showed any reflexes related to the presence of the mentioned above metal oxide phases.

The type of Ti-species as well as their aggregation in PCHs was studied by UV–vis-DR spectroscopy. Fig. 4 shows spectra obtained for a series of the samples with various contents of titanium (PCH-1.5Ti, PCH-7.5Ti and PCH-15Ti). It should be mentioned that these spectra are the results of the subtraction of the spectra recorded for the PCH sample from the spectra of the Ti-containing sample. Therefore, the spectra presented in Fig. 4 are related only to the titanium present in the PCH samples. The spectra were deconvoluted into three bands. The first band is located for all the samples in the range of 200–220 nm and could be assigned to the presence of Ti^{4+} ions in the tetrahedral coordination (i.e. titanium incorporated into the framework of the silica matrix). These bands are a result of charge transition in $[TiO_4]$ and $[O_3Ti–OH]$ moieties [22–24]. The bands centred at about 230–240 nm are assigned to the isolated extraframework Ti^{4+} cations in the octahedral coordination. Partially polymerized hexacoordinated Ti-species, which contain Ti–O–Ti bridges and belong to a silicon-rich amorphous phase, would exhibit a band at about 260–270 nm [25]. Bands characteristics for anatase clusters expected at about 330 nm [22] were not found.

Deconvolution of the bands shows that titanium in the PCH samples is present mainly in the form of in the hexacoordinated and tetracoordinated Ti cations as well as partially polymerized Ti-species.

Transition metals (Cu, Fe) were deposited on the surface of the PCH materials using an ion-exchange method. Nearly the same loading of copper oxide (1.97–2.19 wt. %) was found in all the PCH samples doped with this metal. The content of iron oxide in the Fe-modified samples was much higher and varied in the range of 7.00–7.61 wt. %. However, it should be noted that iron is a natural component of the raw clay (cf. Table 1). Fig. 5 shows the UV–vis-DR spectra of the samples modified with copper and iron. It should be mentioned that also these spectra are the results of the subtraction of the spectra recorded for the PCH support from the spectra of this support modified with transition metal. Therefore, the spectra presented in Fig. 5 are related only to the deposited transition metals.

The spectra obtained for the Cu-containing samples were deconvoluted into two bands centred at about 250–270 and 340–355 nm. The first peak is attributed to the charge-transfer between the mononuclear Cu^{2+} ion and oxygen, while the band at 340–355 nm can be ascribed to the charge-transfer between Cu^{2+} and oxygen in the oligonuclear $[Cu–O–Cu]_n$ species [26]. It should be noted that in the studied samples, copper exist mainly in the form of isolated species. For the Ti-containing clays, the intensity of peak related to the surface oligonuclear $[Cu–O–Cu]_n$ clusters increased.

The spectra obtained for the Fe-modified samples were deconvoluted into three bands. The peaks centred at about 210–230 nm are related to the presence of isolated Fe^{3+} cations in the tetrahedral coordination, while the band at about 260–300 nm is attributed to the mononuclear Fe^{3+} ions in the octahedral coordination [27–29]. The range of 300–400 nm is characteristic of the bands assigned to the small oligonuclear Fe_xO_y clusters [30]. There were not detected any band above 400 nm related to the bulky Fe_2O_3 clusters [31]. Comparison of the band intensities lead to the conclusion that iron was deposited mainly in the form of the mononuclear Fe^{3+} ions in the octahedral coordination and the small oligonuclear Fe_xO_y clusters. For the Ti-containing PCHs, the higher contribution of iron in the form of the small oligonuclear Fe_xO_y clusters was found.

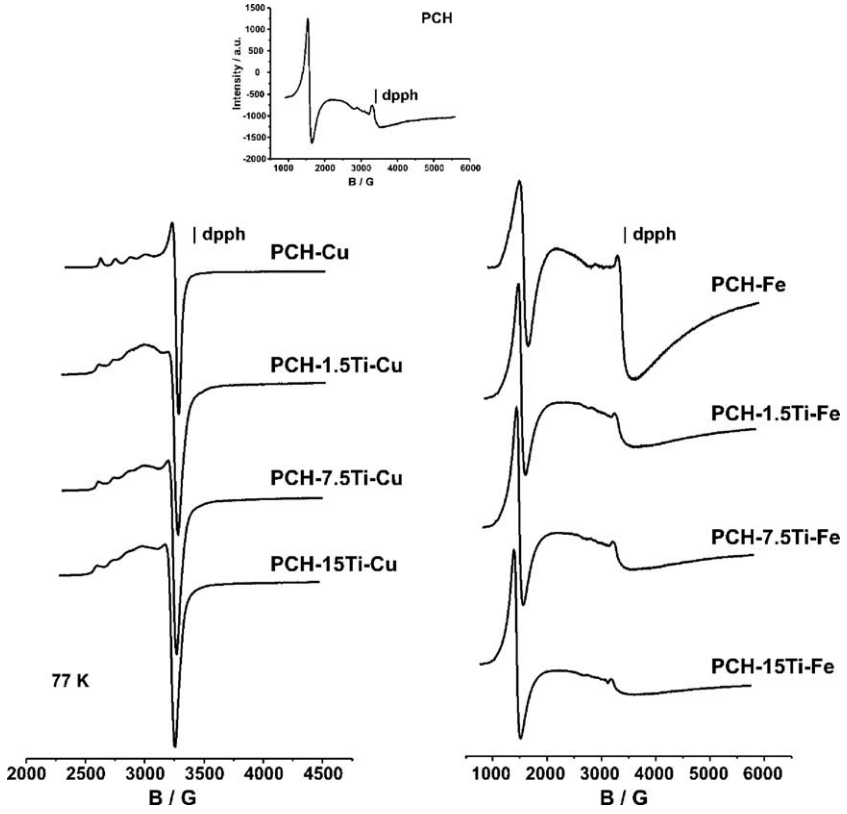

Fig. 6. Low temperature (196 °C) EPR spectra of PCH-Ti-Cu and PCH-Ti-Fe samples of various Ti loading. In the insert, an EPR spectrum of an undoped PCH sample is shown.

Reported above, information about the status of copper and iron ions, present mainly as isolated species in the investigated Cu- and Fe-modified samples, derived from electronic spectra, were confirmed also by EPR results. The corresponding spectra, recorded at −196 °C, are shown in Fig. 6. The shape of the spectra obtained for Cu- and Fe-containing PCHs was characteristic of $3d^9$ (Cu^{2+}, $S = 1/2$) and high-spin $3d^7$ (Fe^{3+}, $S = 5/2$) ions, magnetically isolated in oxygen local environment. Distribution of these dopants in the structure of the studied material was quite homogeneous as it can be inferred from the presence of just one type of the EPR signal, contributing to all spectra recorded for Fe- and Cu-loaded samples, respectively. It was especially well visible in the case of an axial

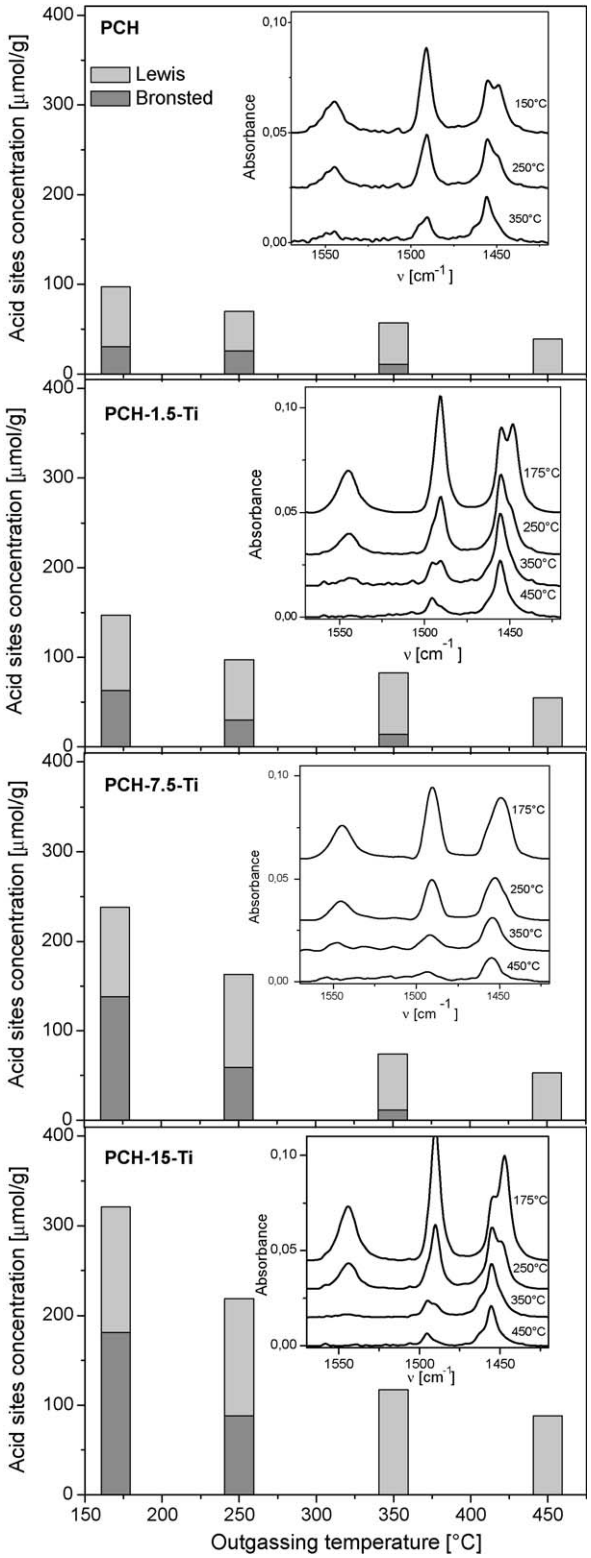

Fig. 7. Concentration of surface acid sites determined for a series of the PCH samples. In the inserts, FT-IR spectra of the samples pre-adsorbed with pyridine.

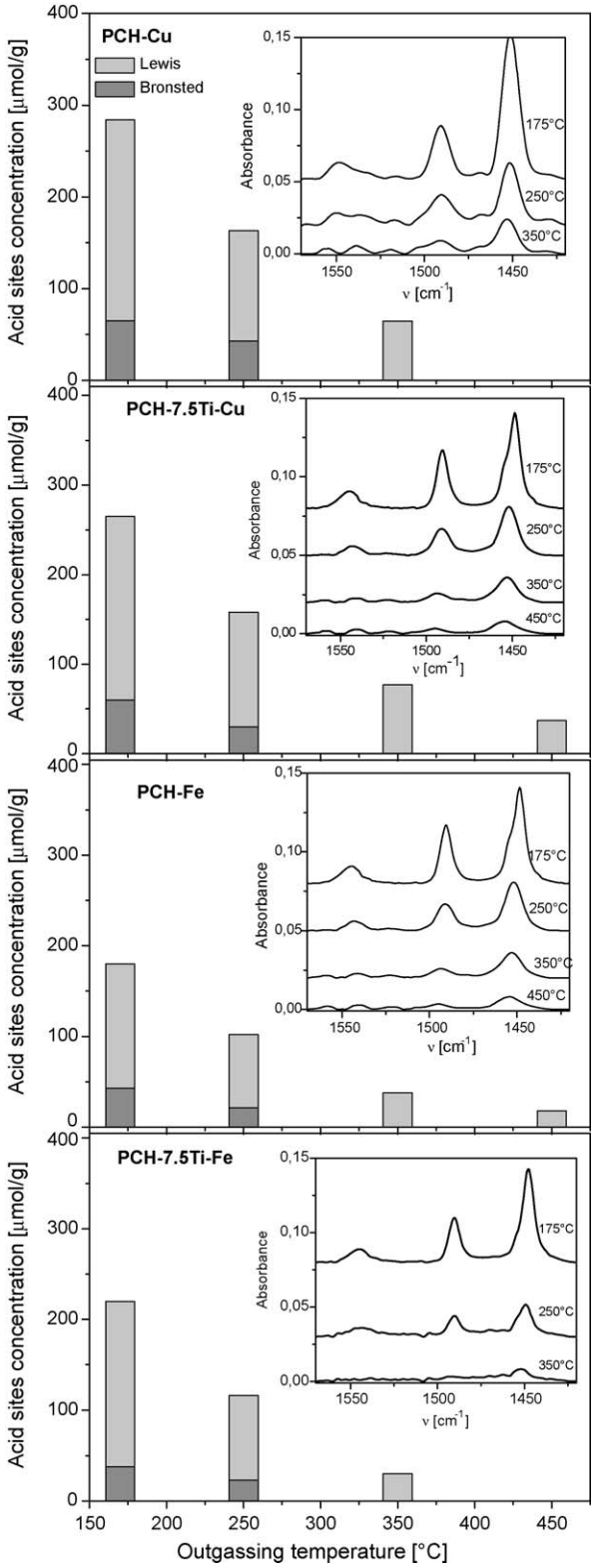

Fig. 8. Concentration of surface acid sites determined for the samples doped with copper and iron. In the inserts, FT-IR spectra of the samples pre-adsorbed with pyridine.

spectrum obtained for PCH-Cu sample, where just one set of well resolved four-fold hyperfine (hfs) lines ($|A_{||}| \approx 123$ G), occurring due to interaction of an unpaired electron with ^{63}Cu (nat. abund. 69.09%) and ^{65}Cu (nat. abund. 30.91%) nuclei of spins $I = 3/2$, was observed. Basing on the relationship between spin Hamiltonian parameters determined directly from PCH-Cu spectrum: $g_{||} \approx 2.41$ and $g_{\perp} \approx 2.07$ (*i.e.* $g_{||} > g_{\perp} > g_e = 2.0023$), copper ions can be localized in the tetragonally elongated octahedral, square planar (D_{4h}) or square pyramidal (C_{4v}) environments [32,33]. In the case of Fe-modified PCHs, the predominant, almost isotropic, signal at $g \approx 4.26$ is characteristic of Fe^{3+} ions isolated in rhombically distorted environment (ZFS parameters $|E/D| = 1/3$) [34,35]. The intensity of the spectrum of PCH-Fe sample was almost two times higher, in comparison to that recorded for a raw PCH material (Fig. 6, inset), where iron ions naturally occurred in the same lattice positions. Relatively high intensity of a signal at $g \approx 2.00$ in the spectrum of PCH-Fe, visible also as a weak line in the EPR spectrum of the raw PCH, and attributed to the high-spin Fe^{3+} ions occupying positions of relatively high symmetry ($E \approx 0$) [36], can be explained by an occurrence of structural distortion of the local symmetry, involved by an intentional doping of PCH material with iron dopant. When titanium ions are present in PCH structure such effect seems to be eliminated and the intensity of the signal at $g \approx 2.00$ is of the same level as observed in the spectrum of raw PCH, taking as a measure intensity ratio of the lines at $g \approx 2.00$ and that at $g \approx 4.26$.

Presence of titanium ions in PCH-Cu structure resulted in the partial agglomeration of the Cu^{2+} ions, which can magnetically interact within surface oligomers, giving rise to the structureless, axial EPR signals, contributed to the presented spectra (Fig. 6). Such signals overlap previously described one, attributed to the isolated Cu^{2+} species. In consequence, partial disappearance of the resolved hfs lines can be observed. In parallel, structural changes occurring in Ti-containing systems can be responsible for localization of at least a part of Cu^{2+} ions in new environments of slightly distorted local geometries, in comparison to that characteristic of PCH-Cu system. Such effect can also contribute to the observed changes in the hyperfine structure of spectra of PCH-Ti-Cu samples. The signals from Fe^{3+} did not exhibit any hfs, thus only the slight broadening of the spectral, due to progressive dipole–dipole interaction among the paramagnetic Fe^{3+} species, can be an evidence for changes in iron speciation analogous as described earlier for copper ions.

The surface acidity of the PCHs was studied by FT-IR analysis of the samples pre-adsorbed with pyridine. Pyridine was adsorbed at 170 °C in all PCHs (activated at 550 °C) and subsequently desorbed at the adsorption temperature for 20 min to remove weakly bonded pyridine molecules. The amount of Brønsted sites (OH groups other than silanols) was calculated from the intensity of the 1540 cm^{-1} PyH^+ pyridinium ions band and its absorption coefficient equal to 0.078 cm/μmol, as determined in our previous studies [37]. Similarly, the number of coordinated pyridine molecules (pyridine bonded onto Lewis sites, PyL) can be determined from the intensity of the 1450 cm^{-1} band and its absorption coefficient equal to 0.165 cm/μmol [38]. Only the intensities of the bands were taken for the calculations because in most of the PCH samples silanol groups are interacting with pyridine quite strongly and the band of hydrogen-bonded pyridine overlaps with the band of pyridine bonded on Lewis sites. In each case, the band fitting procedure was carried out (results not shown for the sake of clarity) to discriminate between those two forms of chemisorbed pyridine.

The results are summarized in Fig. 7. The PCH sample contains both Lewis and Brønsted acid sites, however the former are much stronger than the latter. The ≡Si–O–Al≡ bridges bond the octahedral alumina sublayer and tetrahedral silica sheet of montmorillonite. Therefore, the ≡Si–OH–Al≡ Brønsted acid sites can be exposed only on the edges of the montmorillonite crystallites. Lewis acid sites exist in the PCH sample due to the presence of aluminium in the octahedral sublayer of montmorillonite. Probably, the presence of transition metal cations (Fe^{3+}, Ti^{4+}) incorporated into the structure of the clay layers also generated the Lewis-type acidity. Presence of the acid centers on the surface of the pure silica pillars is rather improbable. Introduction of titanium into the PCH structure resulted in a significant increase of the concentration of both Brønsted and Lewis acid sites (Fig. 7).

Thermodesorption of pyridine was followed by FT-IR to estimate the acid strength of both Brønsted and Lewis acid centres. The position of the IR bands of chemisorbed pyridine is independent on the strength of the site, and depends only on the type of bonding, therefore the relative intensities of the bands of

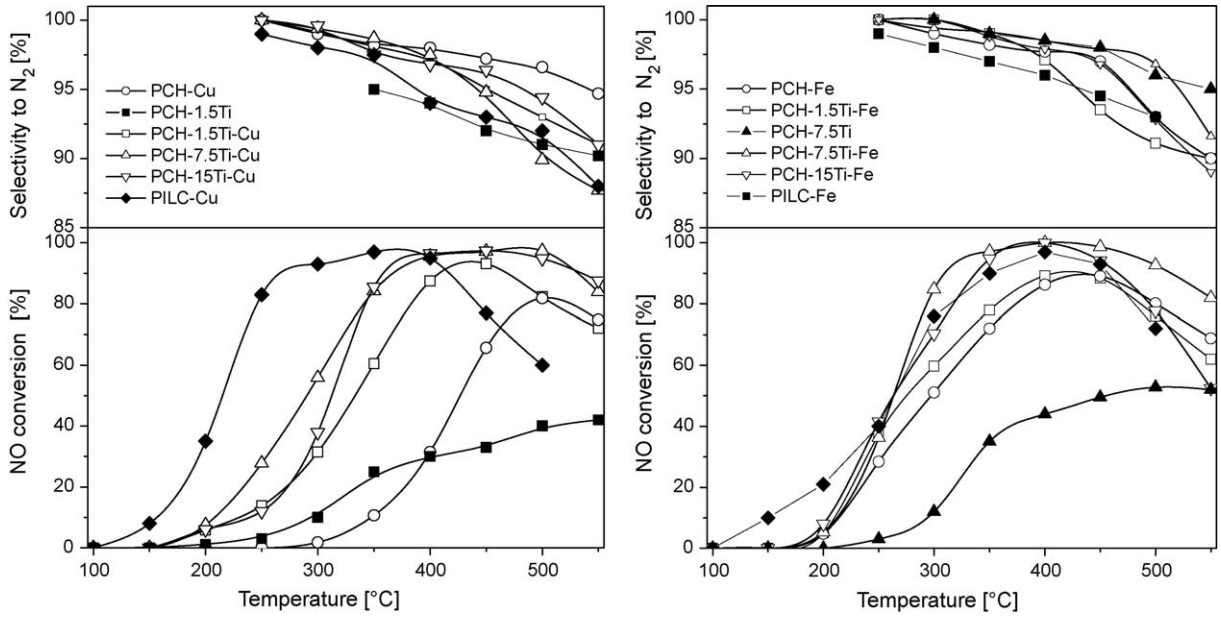

Fig. 9. Results of catalytic tests for the PCH samples modified with copper and iron.

pyridine and not their frequencies were taken to estimate the relative acid strength of the acidic sites in the examined clays. It was shown (cf. Fig. 7) that the amount of pyridine adsorbed on Brønsted sites (calculated from the intensity of the 1545 cm^{-1} PyH^+ band) decreased monotonically with the desorption temperature. At the same time, the amount of coordinatively bonded onto Lewis centres pyridine (calculated from the intensity of the 1454 cm^{-1} PyL band) remained virtually constant suggesting that Lewis-type centres are stronger than the Brønsted ones. In the case of the Ti-modified PCH samples acid sites are located not only on the surface of the clay layers but also on the silica-titania pillars. An increased Brønsted acidity of the Ti-containing PCH samples is related to the presence of Ti^{4+} cations in tetrahedral and octahedral coordinations located on the surface of pillars. Tanabe et al. [39] suggested that Ti cations of coordination number four are the source of the Lewis acidity, while those of coordination number six, can be a source of the Brønsted acidity. For the latter case, the excess of the negative charge of −2 is distributed on six Ti–O bonds and should generate Brønsted acidity. It should be noted that titanium in tetrahedral and octahedral coordinations were found in UV–vis-DRS measurements for all the Ti-containing samples (cf. Fig. 4).

Deposition of transition metals (Cu, Fe) by an ion-exchange method resulted in a disappearance of the Brønsted-type acid sites and formation of the Lewis acid centres (Fig. 8). This effect is related to the exchange of protons (from ≡Si–OH–Al≡ bridges, being Brønsted acid sites) for transition metal cations (Cu^{2+} or Fe^{3+}), which can coordinatively bond pyridine. The concentration of these acid sites is comparable for all the Cu-doped samples, however the Cu-modified catalysts based on the Ti-containing PCHs are characterized by the stronger acid centres than the Cu-modified PCH. An opposite effect was found for the Fe-modified samples. The Ti-containing catalysts presented higher concentration of acid sites but of the lower strength than the samples based on the PCH support. Ti-modified PCHs doped with iron contained both Lewis and Brønsted acid centres.

The PCH samples were tested in the role of catalysts for the selective catalytic reduction of NO with ammonia (NO-SCR, DeNO*x*). Nitrogen and water vapour are desired products of this process, while N_2O is undesired side-product. The results of the studies performed for the PCH supports and their modifications with transition metals are presented in Fig. 9. For comparison, the results of the catalytic tests performed for titanium pillared montmorillonite doped with copper (PILC-Cu) and iron (PILC-Fe) are shown. Detailed description of the synthesis of these samples and their characteristics were presented in our previous papers [11,12]. In a series of the Cu-modified samples significant differences between activity of the catalysts based on PILC-Cu, Cu-Ti-conatining PCHs and the PCH-Cu sample were observed.

The DeNO*x* reaction started at temperature about 250 °C in the presence of the PCH-Cu catalyst, while for the Cu-Ti-containing PCHs the NO conversion was detected at temperature about 150 °C and for PILC-Cu at temperature as low as 100 °C. However, it should be noted that in the presence of the PILC-Cu catalyst, the NO conversion decreased due to the competitive ammonia oxidation at temperature above 400 °C. Therefore, the application of this catalyst is limited only to the low or medium temperature DeNO*x* process. The Cu-Ti-containing PCH materials were found to be much more effective catalysts in the high temperature range. In this series of the PCH samples, the best catalytic activity was manifested by PCH-7.5Ti-Cu. It should be noted a very high effectiveness of the DeNO*x* process at temperatures as high as

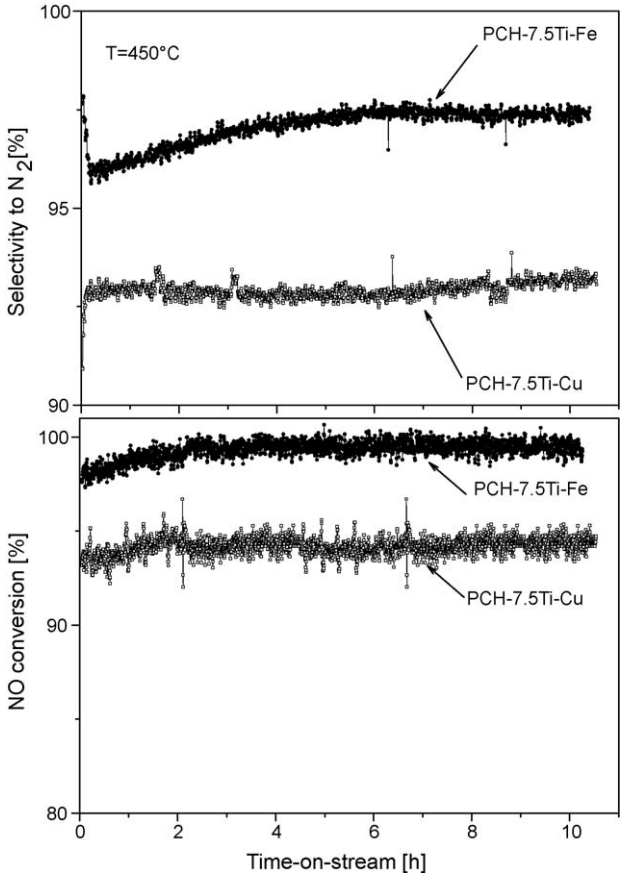

Fig. 10. Stability tests of DeNO*x* process for PCH-7.5Ti-Cu and PCH-7.5Ti-Fe.

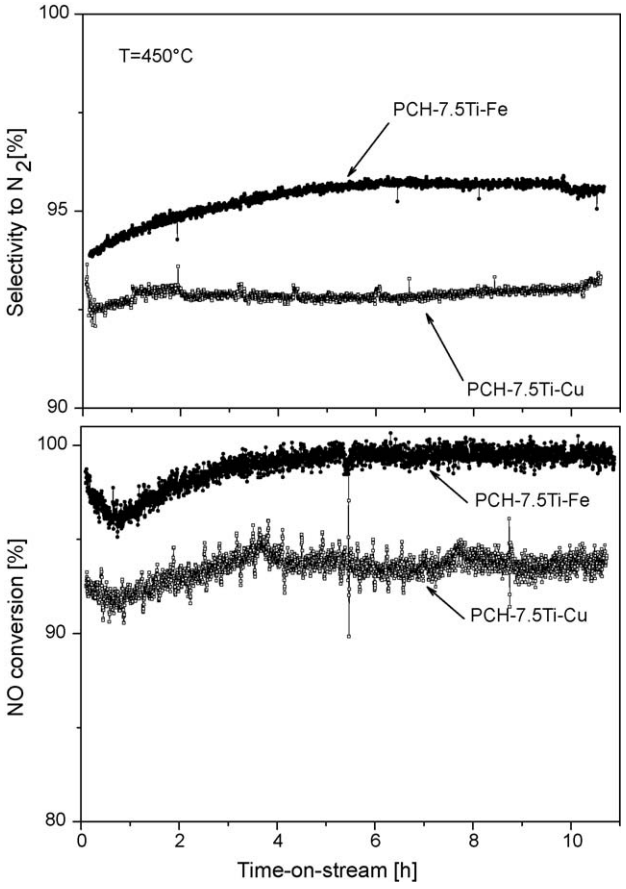

Fig. 11. Stability tests of DeNO*x* process in the wet reaction mixture for PCH-7.5Ti-Cu and PCH-7.5Ti-Fe.

550 °C for the samples with high loading of titanium (PCH-7.5Ti-Cu, PCH-15Ti-Cu). The more, their performance was only slightly limited by the side process of direct ammonia oxidation by oxygen. The selectivity to N_2 was very high and did not drop below 95% at temperatures lower than 450 °C. At higher temperatures selectivity to nitrogen is higher for PCH-15Ti-Cu than for PCH-7.5Ti-Cu. Such significant differences in the catalytic performance of the Cu-modified PCH samples are probably related to the surface acidity as well as to the various forms of the deposited copper species. The less active PCH-Cu sample contained both isolated copper cations as well as oligomeric copper oxide clusters. For the more active Cu-Ti-modified PCH catalysts the contribution of copper in the form of the oligomeric clusters was higher (cf. Fig. 5). Clusters of copper oxides were reported to be more active in the low temperature DeNO*x* process, while isolated Cu^{2+} cations are probably responsible for the activity in the high temperature NO_x reduction and, contrary to aggregated copper oxide species, are less active in the side process of ammonia oxidation [40]. PCH-Cu, which presented the lowest activity in this series of the samples, was characterized by the absence of the strong Lewis acid sites, which were found in the more active Ti-modified catalysts (cf. Fig. 8). For majority of the DeNO*x* catalysts the Eley–Rideal mechanism including the reaction between chemisorbed ammonia species and gaseous or weakly bonded NO was suggested [e.g. [41–43]]. It seems that the PCH sample did not contain acid sites strong enough to activate ammonia molecules in the high temperature range. Such strong acid sites are generated by the introduction of titanium into the silica pillars of the PCH materials.

All the Fe-modified PCH samples have shown activity in the DeNO*x* process in a very similar temperature range, however their effectiveness in this process was different. The following order of the activity in this group of the catalysts at temperature 350 °C was found: PCH-7.5Ti-Fe > PCH-15Ti-Fe > PILC-Fe > PCH-1.5Ti-Fe > PCH-Fe. At higher temperatures the competitive reaction of ammonia oxidation by oxygen decreased the NO conversion and selectivity to N_2. This effect was more distinct for PCH-15Ti-Fe than for the other catalysts.

The differences in the catalytic performance observed in a series of the Fe-modified samples are probably related to various distributions of the surface forms of iron and surface acidity. The catalysts based on Fe-Ti-modified PCHs were characterized by larger contribution of iron in the form of oligomeric metal oxide clusters than the PCH-Fe sample. Iron cations in such oligomeric clusters can be reduced at lower temperatures than isolated Fe^{3+} ions [44,45]. Therefore, it could be expected that the samples with larger contribution of such species should be more active at lower temperatures. On the other hand the oligomeric iron oxide species are known to be more active in ammonia oxidation than isolated Fe^{3+} cations [44–46]. Surface acidity is another feature of the samples, which may influence their catalytic performance. The catalysts based on Fe-modified PCHs contain both Lewis and Brønsted acid sites. However, it should be noted that the more active catalysts based on Ti-modified PCHs are characterized by the higher concentration of surface acid sites than the PCH-Fe catalyst. Therefore, the surface concentration of acid sites, besides their type and strength, is another feature of the samples, which can influence their catalytic performance.

It should be noted that the catalytic activity of the Ti-containing PCH supports (non-modified with transition metals) is significantly lower than the samples doped with iron or copper (cf. Fig. 9). Therefore, it seems that the presence of these transition metals is responsible for high activity of the PCH based catalysts.

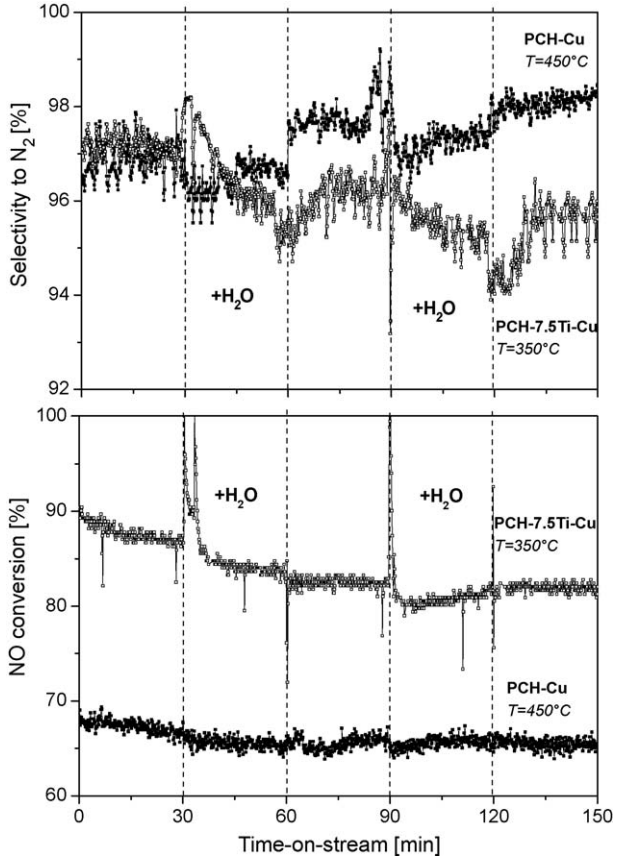

Fig. 12. Study of influence of water vapour on catalytic activity of PCHs modified with copper.

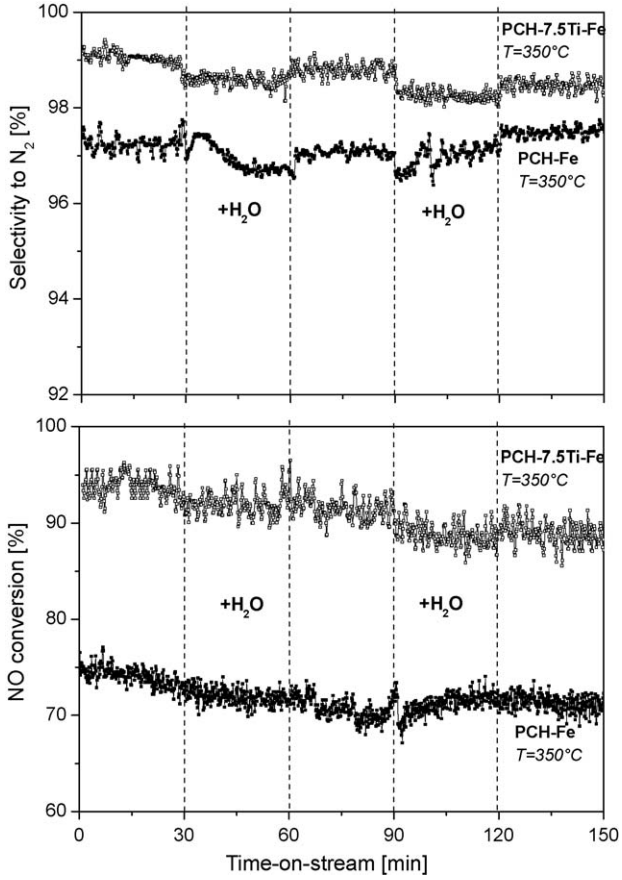

Fig. 13. Study of influence of water vapour on catalytic activity of PCHs modified with iron.

Additional stability tests were performed in a flow dry (Fig. 10) or wet (Fig. 11) reaction mixtures at temperature 450 °C for the PCH-7.5Ti-Cu and PCH-7.5Ti-Fe catalysts. It should be noted that during more then 10 h of the catalytic tests only small fluctuations in the NO conversion and the selectivity to nitrogen were observed.

Additionally, the influence of water vapor on the catalytic performance of the Cu- and Fe-doped samples was studied by a periodical addition of steam into the reaction mixture. The results of these isothermal tests performed for the Cu- and Fe-modified samples are presented in Figs. 12 and 13, respectively. An addition of water vapor (~5.0 vol.%) into the reaction mixture resulted in a slight decrease in the NO conversion and selectivity to nitrogen. In a series of the Cu-doped catalysts the most significant decrease of the NO conversion (~ 4%) and selectivity to N_2 (~2.5%) was observed for PCH-7.5Ti-Cu. The other Cu-modified samples were less affected by the introduction of steam into the reaction mixture. In general, the Fe-doped catalysts were found to be less sensitive for the water vapor presence (Fig. 13). In this series of the samples the drop of the NO conversion and selectivity to N_2 was lower than 3 and 1.5%, respectively.

It should be noted that effect of water vapor addition has not resulted in a permanent deactivation of the catalysts and the exchange from wet to dry reaction mixture resulted in a full or partial reactivation of the catalysts. Therefore, it seems that the competition of water and ammonia molecules for the same adsorption sites was the main reason of the observed small decrease in the NO conversion and selectivity to N_2. In order verify this hypothesis additional NH_3-TPD experiments were performed. Ammonia was adsorbed on the outgased samples or the samples pretreated with water vapor. The comparison of NH_3-TPD results is presented in Fig. 14. It could be seen that adsorbed water limited the surface concentration of ammonia adsorbed in the next step. Therefore, these results supports hypothesis that competition of ammonia and water for these same adsorption sites is responsible for decrease in the NO conversion in the wet conditions.

Apart from water vapor also sulfur dioxide is often responsible for the deactivation of the DeNO*x* catalysts. The studies of the SO_2 influence on the catalytic performance of the PCH-based catalysts doped with Cu or Fe are presented in Figs. 15 and 16, respectively. The activity and selectivity of the PCH-Cu samples was only slightly affected by SO_2. Both parameters were nearly the same before and after treatment of the catalysts with SO_2. The catalysts based on Ti-containing PCHs were more sensitive for SO_2 poisoning. The NO conversion decreased by about 5%, while no changes in the selectivity to N_2 after treatment of the PCH-7.5Ti-Cu catalyst with sulphur dioxide were observed.

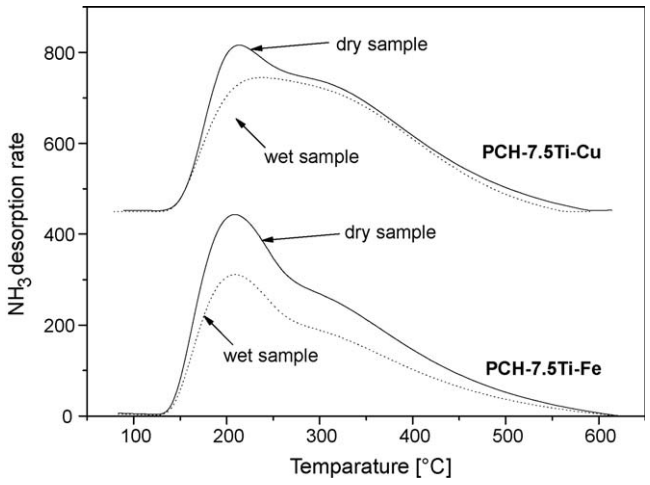

Fig. 14. Results of NH_3-TPD for "dry" samples and catalysts pre-adsorbed with water vapour.

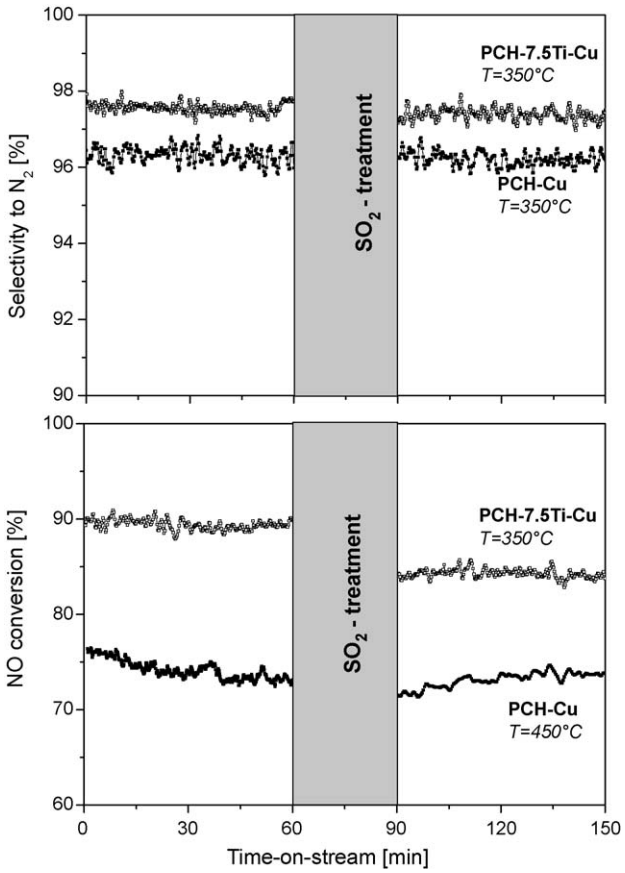

Fig. 15. Study of influence of SO_2 on catalytic activity of PCHs modified with copper.

The Fe-modified PCH samples were found to be less sensitive for the poisoning by sulphur dioxide. The highest deactivation effect was observed for PCH-7.5Ti-Fe, where the NO conversion decreased by about 3%. For the other catalysts of this series, especially for PCH-Fe, the activity was not or only slightly affected by SO_2 treatment.

The commercial the V_2O_5-TiO_2 based DeNO*x* catalysts effectively operate at temperatures 250–400 °C [47]. At higher temperatures the side reaction of ammonia oxidation decreases efficiency of the NO conversion. Analysis of the results of the catalytic tests presented in Fig. 9 shows that the PCH based catalysts, especially those modified with iron, effectively operate at temperatures higher than 400 °C and therefore these materials seems to be interesting candidates for the catalysts of the high temperature DeNO*x* process. The other, intensively studied catalysts for the high temperature DeNO*x* are based on ZSM-5 zeolites. Their catalytic performance was presented in a large number of papers [e.g. [47–50]] and was reported to depend on various parameters (e.g. surface acidity–Si/Al ratio, forms of the deposited transition metals, method used for deposition of active components, precursors of active phase). Long and Yang [49], who studied the activity of ZSM-5 zeolites doped with iron by various methods (aqueous and solid state ion-exchanges, chemical vapor deposition) in the DeNO*x* process showed the high efficiency of the reaction up to temperature as high as 450 °C. At higher temperatures the competitive reaction of ammonia oxidation decreased the NO conversion. Authors suggested that isolated Fe^{3+} cations play a role of active centers. Similar, high temperature activity of ZSM-5 modified with iron by ion-exchange and grafting methods were reported by Delahay et al. [50]. However, in this case authors suggest that iron oxo-species are active sites of the reaction. Comparison of the ZSM-5 and PCH based catalysts

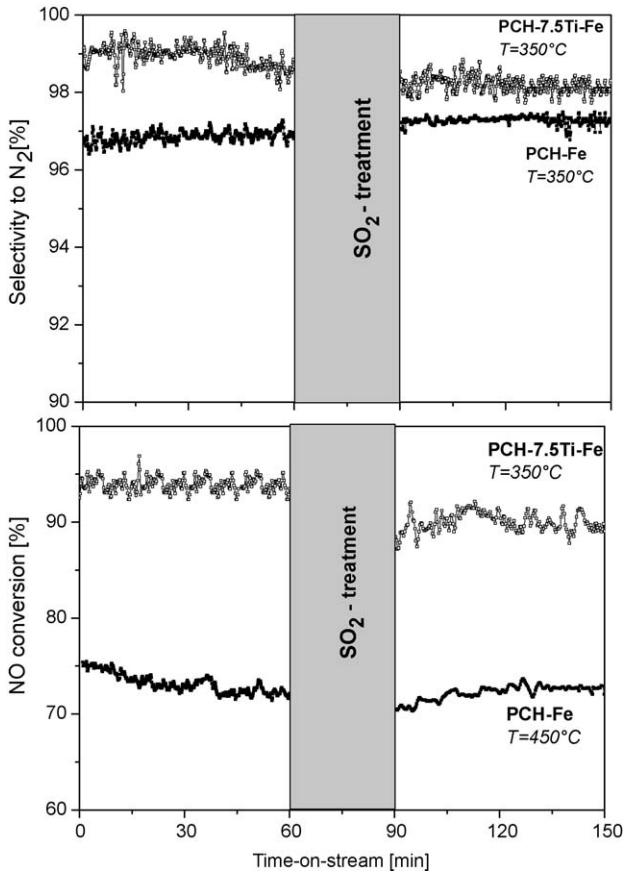

Fig. 16. Study of influence of SO_2 on catalytic activity of PCHs modified with iron.

modified with iron shows that these catalysts present comparable activity in the high temperature DeNO*x* process. Taking into account a very large number of the studies focused on application of the ZSM-5 materials in the DeNO*x* process and only few papers related to the PCH based catalysts, the results obtained for the later ones seem to be very promising.

4. Conclusions

The novel group of the porous clay heterostructures (PCHs) intercalated with silica-titania pillars was synthesized from natural montmorillonite. The incorporation of titanium into the silica pillars significantly increased surface acidity of PCHs by generation of both Lewis and Brønsted acid sites. Titanium introduced into the PCH samples also influenced the type of transition metal surface species formed during deposition of copper and iron. Transition metals deposited on the surface of the PCH supports were found to be in the form of the isolated cations and small oligonuclear metal oxide clusters. However, in a series of Ti-modified PCHs (PCH-1.5Ti, PCH-7.5Ti. PCH-15Ti) the contribution of iron and copper in the form clustered species was higher than in the clay intercalated with pure silica pillars (PCH).

The Ti-containing PCH samples additionally modified with transition metals were found to be significantly more active than the catalysts based on PCHs intercalated with pure silica pillars. The side process of ammonia oxidation, especially in the presence of the Cu-doped catalysts with high loading of titanium (PCH-7.5Ti-Cu and PCH-15Ti-Cu), was observed at temperatures as high as 500 °C. Therefore, these materials seem to be very interesting candidates for the high temperature DeNO*x* process. Additionally, the PCH based catalysts were found to be only slightly deactivated in the presence of water vapour as well as SO_2.

Acknowledgements

Authors acknowledge the Polish Ministry of Science for financial support in the frame of project N597 150 32/4091 and S&B Industrial Minerals GmbH for supplying of montmorillonite.

References

[1] S. Steinbach, J. Grunwald, U. Gluckert, T. Sattelmayer, Top. Catal. 42–43 (2007) 99.
[2] D.E.W. Vaughan, L.J. Lussier, J.S. Magee, U.S. Pattent 4, 176,090 (1979).
[3] D.E.W. Vaughan, L.J. Lussier, J.S. Magee, U.S. Pattent 4, 248,739 (1981).
[4] D.E.W. Vaughan, L.J. Lussier, J.S. Magee, U.S. Pattent 4, 271,043 (1981).
[5] R.T. Yang, J.P. Chen, E.S. Kikkinides, L.S. Cheng, J.E. Cichanowicz, Ind. Eng. Chem. Res. 31 (1992) 1440.
[6] R.Q. Long, R.T. Yang, Appl. Catal. B 27 (2000) 87.
[7] R.Q. Long, R.T. Yang, J. Catal. 199 (2000) 22.
[8] R.Q. Long, R.T. Yang, J. Catal. 186 (1999) 254.
[9] L. Chmielarz, R. Dziembaj, T. Grzybek, J. Klinik, T. Łojewski, D. Olszewska, H. Papp, Catal. Lett. 68 (2000) 95.
[10] L. Chmielarz, R. Dziembaj, T. Łojewski, A. Węgrzyn, T. Grzybek, J. Klinik, D. Olszewska, Solid State Ionics 141–142 (2001) 715.
[11] L. Chmielarz, P. Kuśtrowski, M. Zbroja, A. Rafalska-Łasocha, D. Dudek, R. Dziembaj, Appl. Catal. B 45 (2003) 103.
[12] L. Chmielarz, P. Kuśtrowski, M. Zbroja, W. Łasocha, R. Dziembaj, Catal. Today 90 (2004) 43.
[13] A. Galarneau, A. Barodawalla, T.J. Pinnavaia, Nature 374 (1995) 529.
[14] L. Chmielarz, P. Kuśtrowski, M. Drozdek, R. Dziembaj, P. Cool, E.F. Vansant, Catal. Today 119 (2007) 181.
[15] L. Chmielarz, P. Kuśtrowski, Z. Piwowarska, B. Dudek, B. Gil, M. Michalik, Appl. Catal. B 88 (2009) 331.
[16] L. Chmielarz, B. Gil, P. Kuśtrowski, Z. Piwowarska, B. Dudek, M. Michalik, J. Solid State Chem. 182 (2009) 1094.
[17] L. Chmielarz, R. Dziembaj, T. Grzybek, J. Klinik, T. Łojewski, D. Olszewska, A. Węgrzyn, Catal. Lett. 70 (2000) 51.
[18] S.J. Greek, K.S.W. Sing, Adsorption, Surface Area and Porosity, Academic Press, London, 1982.
[19] G.W. Brindley, R.W. Hoffmann, Clays Clay Miner. 9 (1962) 546.
[20] S. Xu, S.A. Boyd, Langmuir 11 (1995) 2508.
[21] L.V. Duong, T.J. Kloprogge, L.R. Frost, J.A.R. van Veen, J. Porous Mat. 14 (2007) 71.
[22] Y. Segura, L. Chmielarz, P. Kuśtrowski, P. Cool, R. Dziembaj, E.F. Vansant, Appl. Catal. B 61 (2005) 69.
[23] A. Corma, Chem. Rev. 97 (1997) 2373.
[24] T. Blanco, A. Corma, M.T. Navarro, J. Pérez-Parienta, J. Catal. 156 (1995) 65.
[25] X.F. Li, H.X. Gao, G.J. Jin, L. Chen, L. Ding, H.Y. Yang, Q.L. Chen, J. Mol. Struct. 872 (2008) 10.
[26] F.M.T. Mendes, M. Schmal, Appl. Catal. A 151 (1997) 393.
[27] J. Pérez-Ramirez, M.S. Kumar, A. Brückner, J. Catal. 223 (2004) 13.
[28] M.S. Kumar, M. Schwidder, W. Grünet, A. Brückner, J. Catal. 227 (2004) 384.
[29] M.S. Kumar, J. Pérez-Ramirez, M.N. Debbagh, S. Smarsly, U. Bentrup, A. Brückner, Appl. Catal. B 62 (2006) 244.
[30] M.A. Wojtowicz, J.R. Pels, J.A. Moulijn, Fuel Proc. Technol. 34 (1993) 1.
[31] E. Suzuki, K. Nakashiro, Y. Ono, Chem. Lett. (1988) 953.
[32] K. Bahranowski, R. Dula, M. Łabanowska, E.M. Serwicka, Appl. Spectr. 50 (1996) 1439.
[33] L. Trouillet, Th. Toupance, F. Villain, C. Louis, Phys. Chem. Chem. Phys. 2 (2000), 2005.
[34] J.R. Pilbrow, Transition Ion Electron Paramagnetic Resonance, Clarendon Press, Oxford, 1990.
[35] E.A. Zhilinskaya, G. Delahay, M. Mauvezin, B. Coq, A. Aboukaïs, Langmuir 19 (2003) 3596.
[36] J. Pérez-Ramírez, M. Santhosh Kumar, A. Brückner, J. Catal. 223 (2004) 13.
[37] J. Datka, B. Gil, A. Kubacka, Zeolites 18 (1997) 245.
[38] J. Datka, B. Gil, A. Kubacka, Zeolites 17 (1996) 428.
[39] K. Tanabe, T. Sumiyoshi, K. Shibata, T. Kiyoura, J. Kitagawa, Bull. Chem. Soc. Jpn. 47 (1974) 1064.
[40] L. Chmielarz, P. Kuśtrowski, R. Dziembaj, P. Cool, E.F. Vansant, Appl. Catal. B 62 (2006) 369.
[41] H. Schneider, S. Tschudin, M. Schneider, A. Wokaun, A. Baiker, J. Catal. 147 (1994) 13.
[42] E. Tronconi, L. Lietti, P. Forzatti, S. Malloggi, Chem. Eng. Sci. 51 (1996) 2965.
[43] K. Otto, M. Shelef, J. Catal. 18 (1970) 184.
[44] G.J. Golodets, Yu.I. Pyatnitskii, Katal. Katal. 4 (1968) 25.
[45] E.M. Slavinskaya, S.A. Veniaminov, P. Notte, S. Ivanova, A.I. Borowin, Yu.A. Cheslakov, I.A. Polukhina, A.S. Noskom, J. Catal. 222 (2004) 129.
[46] L. Chmielarz, P. Kuśtrowski, A. Rafalska-Łasocha, R. Dziembaj, Appl. Catal. B 58 (2005) 235.
[47] G. Busca, L. Lietti, G. Ramis, F. Berti, Appl. Catal. B 18 (1998) 1.
[48] K. Rahkamaa-Tolonen, T. Maunula, M. Lomma, M. Huuhtanen, R.L. Keiski, Catal. Today 100 (2005) 217.
[49] R.Q. Long, R.T. Yang, Catal. Lett. 74 (2001) 201.
[50] G. Delahay, D. Valade, A. Guzman-Vargas, B. Coq, Appl. Catal. B 55 (2005) 149.